High resolution and low-temperature photoelectron spectroscopy of an oxygen-linked fullerene dimer dianion: $C_{120}O^{2-}$

Xue-Bin Wang,[1,2] Katerina Matheis,[3] Ilya N. Ioffe,[4,a)] Alexey A. Goryunkov,[4] Jie Yang,[1,2] Manfred M. Kappes,[2,3,b)] and Lai-Sheng Wang[1,2,c)]
[1]*Department of Physics, Washington State University, 2710 University Drive, Richland, Washington 99354, USA*
[2]*Chemical and Materials Sciences Division, Pacific Northwest National Laboratory, MS K8-88, P.O. Box 999, Richland, Washington 99352, USA*
[3]*Institut für Physikalische Chemie, Universität Karlsruhe, Kaiserstrasse 12, D-76128 Karlsruhe, Germany*
[4]*Chemistry Department, Moscow State University, Moscow 119992, Russia*

(Received 15 January 2008; accepted 6 February 2008; published online 18 March 2008)

$C_{120}O$ comprises two C_{60} cages linked by a furan ring and is formed by reactions of $C_{60}O$ and C_{60}. We have produced doubly charged anions of this fullerene dimer ($C_{120}O^{2-}$) and studied its electronic structure and stability using photoelectron spectroscopy and theoretical calculations. High resolution and vibrationally resolved photoelectron spectra were obtained at 70 K and at several photon energies. The second electron affinity of $C_{120}O$ was measured to be 1.02 ± 0.03 eV and the intramolecular Coulomb repulsion was estimated to be about 0.8 eV in $C_{120}O^{2-}$ on the basis of the observed repulsive Coulomb barrier. A low-lying excited state ($^2B_1$) was also observed for $C_{120}O^-$ at 0.09 eV above the ground state ($^2A_1$). The $C_{120}O^{2-}$ dianion can be viewed as a single electron on each C_{60} ball very weakly coupled. Theoretical calculations showed that the singlet and triplet states of $C_{120}O^{2-}$ are nearly degenerate and can both be present in the experiment. The computed electron binding energies and excitation energies, as well as Franck–Condon factors, are used to help interpret the photoelectron spectra. A C–C bond-cleaved isomer, $C_{60}-O-C_{60}^{2-}$, was also observed with a higher electron binding energy of 1.54 eV. © *2008 American Institute of Physics*.
[DOI: 10.1063/1.2889384]

I. INTRODUCTION

There has been tremendous interest in the anions of C_{60},[1–4] particularly after the discoveries of conductivity and superconductivity in alkali metal doped fullerenes,[5–8] where not only the isolated electronic structures of the individual fullerene cage but also the cooperative electron-electron and electron-phonon interactions are believed to play important roles.[9–11] $C_{120}O$, consisting of two C_{60} cages linked by a furan ring,[12,13] is a common impurity found in air-exposed samples of C_{60} and formed via reactions of $C_{60}O$ and C_{60}. Its thermal stability[14] and Raman spectra in the condensed phase[15] have been reported. Anions of $C_{120}O$ ($C_{120}O^{n-}$) are common impurities in solutions of C_{60}^{n-} and have been studied by electron paramagnetic resonance (EPR) spectroscopy.[16,17]

The isolated $C_{120}O^{2-}$ dianion is an interesting model system to study spin couplings and electron correlations. There are several important questions: How are the two excess electrons distributed in the molecule? Do they occupy one ball or are they distributed among the two C_{60} fragments? How are the two electrons spin coupled, in a singlet or triplet state? Even though previous EPR studies have detected the triplet state for $C_{120}O^{2-}$, the singlet state is EPR-silent and cannot be studied by EPR. Here we report a low-temperature photoelectron spectroscopy (PES) study of the doubly charged anion $C_{120}O^{2-}$ in the gas phase. Vibrationally resolved photoelectron spectra were obtained and the second electron affinity of $C_{120}O$ was accurately measured. The PES data also yield information about the intramolecular Coulomb repulsion within the doubly charged $C_{120}O^{2-}$. The experimental data are compared with theoretical calculations to aid the spectral assignments and interpretation. The calculations show that the two electrons are distributed on the two C_{60} units separately with relatively weak spin coupling: The singlet and triplet states are predicted to be nearly degenerate and both should be present experimentally. In addition, the gas-phase study provides intrinsic experimental information, which will be valuable to understand the electronic structure and electron-phonon couplings in $C_{120}O$ and its anions, as shown previously for C_{60}^-.[11,18,19]

II. EXPERIMENTAL AND THEORETICAL METHODS

A. Low-temperature photoelectron spectroscopy

The experiment was performed with an electrospray-PES apparatus coupled with a temperature-controlled ion trap.[19,20] The $C_{120}O$ sample was prepared according to Ref. 12 and purified by high-performance liquid chromatography, as described previously.[15] The $C_{120}O^{2-}$ dianion solution was prepared by reducing the neutral molecules using tetrakis(dimethyl-amino)ethylene in a mixed *o*-dichlorobenzene and acetonitrile solvent, similar to the for-

a)Electronic mail: ioffe@thermo.chem.msu.ru.
b)Electronic mail: manfred.kappes@chemie.uni-karlsruhe.de.
c)Electronic mail: ls.wang@pnl.gov.

mation of fullerene dianions.[21,22] The resulting solution was used directly in the electrospray and the $C_{120}O^{2-}$ dianion was readily observed. Anions from the electrospray source were first focused radially and transported axially by a dynamic ion-funnel device.[23] Following the ion-funnel, the anions were guided by a radio-frequency octopole and quadrupole system and then bended 90° into a Paul trap for ion accumulation and cooling. The ion trap was attached to the cold head of a closed-cycle helium refrigerator and its temperatures can be controlled between 10 and 350 K. For the current experiment, the ion trap was operated at 70 K and approximately 0.1 mTorr N_2 was used as the background gas for ion cooling.

The trapped ions were pulsed out into the extraction zone of a time-of-flight mass spectrometer at 10 Hz repetition rate. The ions of interest were mass selected and decelerated before being intercepted by a detachment laser beam in the interaction zone of a magnetic-bottle photoelectron analyzer (the strength of the magnetic field is ~500–800 G in the interaction zone). Four photon energies were used in the current study: 193 nm (6.424 eV) from an ArF excimer laser and 266 nm (4.661 eV), 355 nm (3.496 eV), and 532 nm (2.331 eV) from a Nd:YAG (yttrium aluminum garnet) laser. The laser was operated at 20 Hz repetition rate with the ion beam off at alternate shots for background subtraction. The photodetached electrons were collected with nearly 100% efficiency by the magnetic bottle and analyzed in a 5-m-long electron flight tube. The electron energy resolution was $\Delta E/E \sim 2\%$, i.e., 20 meV for 1 eV electrons. Photoelectron time-of-flight spectra were collected and then converted to kinetic energy spectra, calibrated by the known spectra of ClO_2^- and I^-. The electron binding energy spectra presented were obtained by subtracting the kinetic energy spectra from the detachment photon energies.

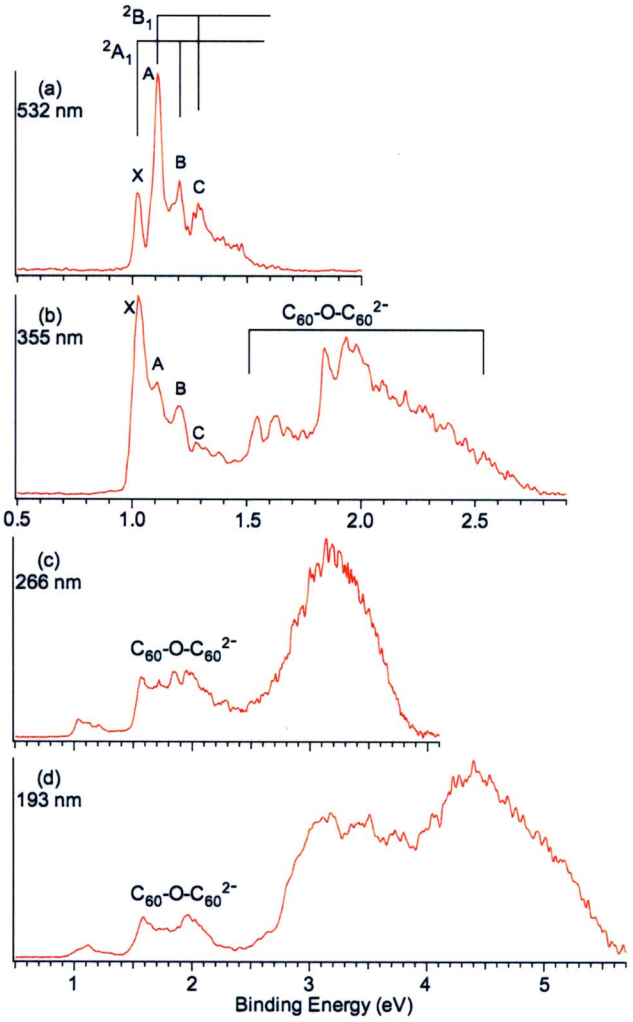

FIG. 1. (Color online) Photoelectron spectra of $C_{120}O^{2-}$ at (a) 532 nm (2.331 eV), (b) 355 nm (3.496 eV), (c) 266 nm (4.661 eV), and (d) 193 nm (6.424 eV). The vertical lines in (a) represent vibrational features. Signals due to a C–C cleaved isomer (C_{60}–O–C_{60}^{2-}) are labeled.

B. Theoretical methods

The density functional theory (DFT) calculations were carried out using the PRIRODA package,[24,25] which utilizes a particularly fast implementation of the resolution-of-the-identity technique. The built-in TZ2P basis set $((11s6p2d)/[6s3p2d]$ for the second row atoms) and the Perdew–Burke–Ernzerhof exchange correlation functional of the generalized gradient approximation type[26] were used. All the species considered were subjected to full geometry optimization at the DFT level of theory without any symmetry constraints. The second electron affinity (i.e., the adiabatic electron detachment energy of the dianion) was calculated as Δ_{KS} between the respective optimized stationary points and further downshifted by 0.2 eV, as was suggested by testing the computational protocol on the set of the dianionic fullerenes measured in Refs. 27 and 28. The excited states of the $C_{120}O^-$ monoanion were calculated using the time-dependent DFT (TDDFT) methodology implemented in the PRIRODA package; the excitation energies obtained were shifted by +0.35 eV on the basis of the simulation of the PES spectra from Ref. 27. The simple single-point multiconfiguration self-consistent-field (MCSCF) calculations were performed with the aid of the PC-GAMESS package.[29] The Frank–Condon factor simulations were carried out using the MOLFC program.[30,31]

III. EXPERIMENTAL RESULTS

We observed three main anions from our electrospray source with about the same abundance in the mass spectrum: C_{60}^-, $C_{60}O^-$, and $C_{120}O^{2-}$. The identity of C_{60}^- and $C_{60}O^-$ was confirmed by their respective photoelectron spectra.[18,32] The $C_{120}O^{2-}$ anions of interest, which appeared between the C_{60}^- and $C_{60}O^-$ peaks in the mass spectrum, were mass selected and photodetached at several photon energies. Figure 1 displays the photoelectron spectra of $C_{120}O^{2-}$ at 532, 355, 266, and 193 nm. Four well-resolved peaks were observed at 532 nm and labeled as X, A, B, and C [Fig. 1(a)] with peak A as the most intense peak. The peak widths of X and A were both 35 meV [full width at half maximum (FWHM)], close to the instrumental resolution. The electron binding energies measured from the four peaks are 1.02 eV (X), 1.11 eV (A), 1.20 eV (B), and 1.28 eV (C). Peak X represents the transition from the ground state of the $C_{120}O^{2-}$ dianion to that of

the $C_{120}O^-$ monoanion. Its 1.02 eV electron binding energy, which defines the electron affinity of $C_{120}O^-$ or the second electron affinity of $C_{120}O$, suggests that the $C_{120}O^{2-}$ dianion is electronically stable.

At 355 nm [Fig. 1(b)], X, A, B, and C peaks were still resolved, but their relative intensities changed markedly. In particular, the relative intensity of peak X increased significantly, whereas that of peak A decreased. This observation suggested that X and A represented two distinct electronic transitions, which exhibited different photon energy dependent detachment cross sections. Additionally, more spectral features were observed in the 355 nm spectrum beyond 1.5 eV. It should be noted that these high binding energy features were missing in the 532 nm spectrum due to the repulsive Coulomb barrier (RCB), which is a characteristic of photodetachment from multiply charged anions.[33,34] The RCB, which derives from the superposition of the long-range Coulomb repulsion between the outgoing electron and the remaining monoanion and its short-range binding in the dianion, prevents slow electrons from being emitted, resulting in the spectral cutoff at the higher binding energy side (low electron kinetic energies). The spectral cutoff in the 532 nm occurred at ~1.5 eV, which yielded a RCB height of ~0.8 eV (photon energy minus the cutoff energy).

At 266 and 193 nm [Figs. 1(c) and 1(d)], very intense features were observed above 2.6 eV. These features appeared almost continuous due to the expected high density of electronic states. Comparisons of the spectra at 355, 266, and 193 nm indicate clear spectral cutoffs in the high binding energy side in the spectra of 355 nm at ~2.7 eV and 266 nm at ~3.8 eV, which yield RCB heights consistent with that estimated from the cutoff in the 532 nm spectrum.

IV. THEORETICAL RESULTS

A. The ground state of the $C_{120}O^{2-}$ dianion

The geometry of $C_{120}O$ was optimized using DFT. The lowest unoccupied molecular orbital (LUMO) (a_1) and LUMO+1 (b_1) of the neutral $C_{120}O$ molecule are almost degenerate and they are symmetric and antisymmetric with respect to the mirror plane coupling the two fullerene cages, respectively, as shown in Fig. 2. In the $C_{120}O^{2-}$ dianion, the two extra electrons occupy these two orbitals. In addition, DFT calculations predict that the gap between the above mentioned a_1 and b_1 orbitals and the orbitals of the neutral $C_{120}O$ core exceeds 1.2 eV in $C_{120}O^{2-}$, whereas the gap between the a_1 and b_1 orbitals is ~0.1 eV. The DFT geometry optimization of the singlet ($^1A_1$) and triplet ($^3B_1$) states of $C_{120}O^{2-}$ predicted that the singlet state is more stable by 2 kJ/mol. The small energy difference between the singlet and triplet states is not surprising, taking into account the size of the molecule, its almost degenerate orbitals due to two rather weakly interacting equivalent halves, and electron delocalization. Therefore, it is expected that the description of the singlet ground state of $C_{120}O^{2-}$ should also require consideration of the two configurations, namely, both a_1^2 and the b_1^2. Indeed, MCSCF calculations (CASSCF/6-31G with two extra electrons in 12 orbitals approximately corresponding to the doubled set of the triply degenerate LUMO and LUMO+1 of C_{60}) indicate that the ground state ($^1A_1$) wave function is a linear combination of the above configurations, i.e., $0.755(a_1)^2-0.654(b_1)^2$, whereas the calculated low-lying excited triplet state ($^3B_1$) has a configuration of $(a_1)^1(b_1)^1$. With regard to the relative stability of the possible spin states, the MCSCF data are in agreement with the DFT results favoring the singlet state by a negligible margin.

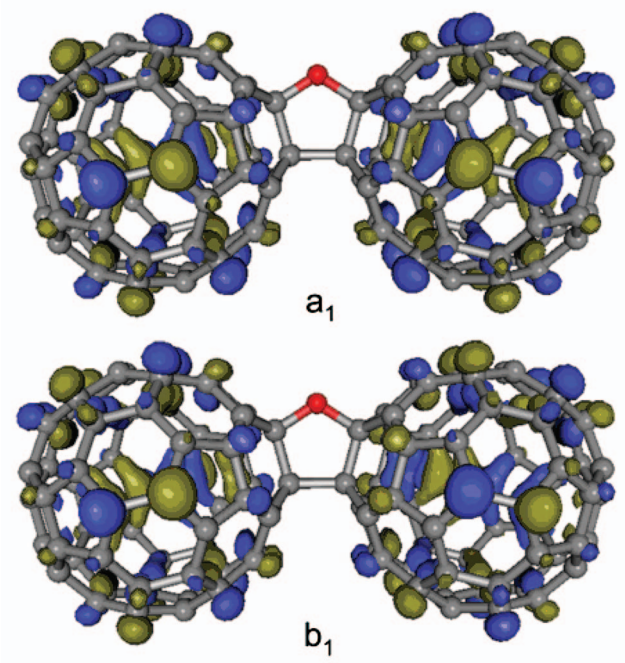

FIG. 2. (Color) Pictures of the lowest unoccupied molecular orbital (LUMO) (a_1) and LUMO+1 (b_1) of $C_{120}O$ drawn with the MOLEKEL visualization package (Ref. 36).

B. Adiabatic detachment energy and band gap

The DFT (Δ_{KS}) calculations of the adiabatic detachment energy of $C_{120}O^{2-}$ give a value of 1.0 eV. Further, TDDFT calculations of the excitation spectrum of the target $C_{120}O^-$ monoanion demonstrate that the states with a hole in the neutral core are separated from the ground state with a singly occupied a_1 orbital by ~1.6 eV.

C. Isomer structural considerations

In order to understand whether the extra negative charge can result in stabilization of structures other than the conventional furan-linked neutral isomer of $C_{120}O$, we also optimized structures with cleaved C–C or C–O bonds in the bridging five-membered furan ring at the DFT level of theory. Even though such structures seem to provide a better basis for accommodation of the two extra electrons in the dianion within a stable singlet state (60 π electrons per fullerene cage in the case of C–C bond being cleaved or 60 π electrons on one cage, 58 π electrons on the other one, and an anionic center on the oxygen atom in the case of C–O bond being cleaved), cleavage of the C–C bond resulted in a structural isomer, which is higher in energy than the furan-linked structure by 35 kJ/mol. Cleavage of the C–O bond

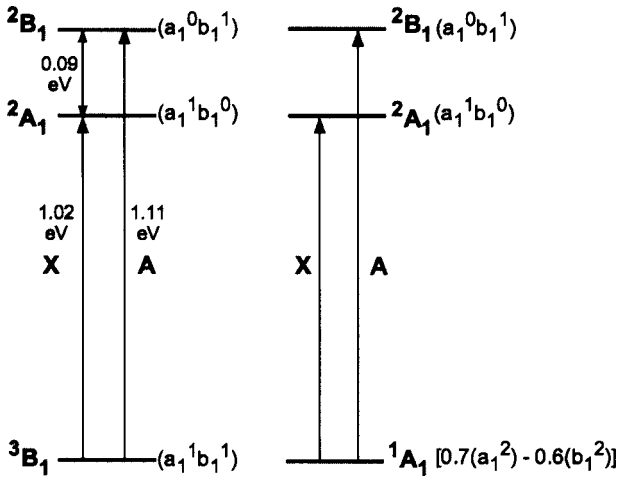

FIG. 3. The first two detachment transitions (X and A) that can derive from the nearly degenerate triplet and singlet states of $C_{120}O^{2-}$, as well as the measured detachment energies.

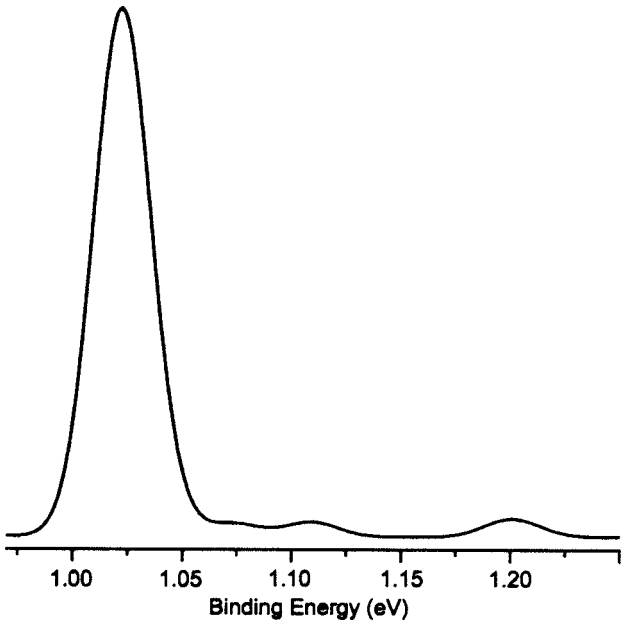

FIG. 4. Franck–Condon factor simulation for the transition between the $^3B_1$ state of $C_{120}O^{2-}$ and the $^2A_1$ state of $C_{120}O^-$. The Franck–Condon factors were convoluted with Gaussians of 0.03 eV FWHM.

was found to be even more unfavorable and the resulting structure is higher by 100 kJ/mol compared to the furan-linked structure. The activation barrier for cleavage of the C–C bond was calculated to be less than 75 kJ/mol.

V. DISCUSSIONS

A. Spin coupling: Is $C_{120}O^{2-}$ singlet or triplet?

The spin state of the $C_{120}O^{2-}$ dianion is interesting and has attracted considerable attentions. EPR spectra indicated a triplet state, while a study using electron spin transient nutation spectroscopy suggested an extremely low separation of only 5 cm^{-1} between the singlet and triplet states for $C_{120}O^{2-}$ in solution.[16,17] Our calculation predicted a small (2 kJ/mol) spin excitation for the isolated dianion. However, it should be noted that for molecular systems of such large size even much more demanding computational methods are unlikely to provide a level of accuracy comparable to the true gap. The theoretical calculations likely overestimated the separation between the singlet and triplet states because we expected that this gap should not change too much in the gas phase relative to that in solution. Thus, even at 70 K, both spin states should be populated in our experiment. However, the 5 cm^{-1} separation between the singlet and triplet states is too small compared to our PES spectral resolution of about 30 meV, and the two spin states can be considered to be degenerate for the purpose of our spectral assignments.

B. Spectral assignments

The calculated adiabatic detachment energy (ADE) of 1.0 eV for $C_{120}O^{2-}$ is in excellent agreement with the observed ground state transition at 1.02 eV, resulting in the $^2A_1$ ground state of $C_{120}O^-$. As shown in Fig. 3, the ground state of $C_{120}O^-$ can be reached from the triplet state of $C_{120}O^{2-}$ by detachment of an electron from the b_1 orbital. The $^2A_1$ ground state of $C_{120}O^-$ can also be reached from the singlet state of $C_{120}O^{2-}$, but the very small energy difference between these transitions cannot be resolved in the current experiment, as mentioned above. Detachment of the electron from the a_1 orbital from the triplet $C_{120}O^{2-}$ resulted in peak A (Fig. 1), corresponding to the first excited state of $C_{120}O^-$ (Fig. 3) with a 0.09 eV excitation energy. The very small excitation energy agrees well with the small gap (0.1 eV) calculated between the a_1 and b_1 orbitals.

The next detachment channels correspond to the detachment from the fully occupied molecular orbitals of the neutral $C_{120}O$ core. TDDFT calculations show that these detachment channels occur at least 1.6 eV below the ground state transition, corresponding to the spectral features above 2.6 eV (Fig. 1). Such spectral pattern is very similar to that of C_{60}^- or $C_{60}O^-$.[18,19,32] Therefore, the B and C features could not be due to distinct low-lying electronic transitions; they are most likely due to vibrational excitations associated with the $^2A_1$ and $^2B_1$ states, as shown in Fig. 1(a). The 0.18 eV spacing (1450 cm^{-1}) between X-B and between A-C is similar to the totally symmetric mode observed in the PES spectra of C_{60}^- or $C_{60}O^-$.[18,19,32] A similar vibration has also been observed in the Raman spectrum of $C_{120}O$ film.[15] This interpretation is confirmed by our calculation of harmonic Frank–Condon factors for the detachment transitions of the triplet $C_{120}O^{2-}$ into the $^2A_1$ ground state of $C_{120}O^-$, as shown in Fig. 4. The lower frequency vibrations for this transition are likely overlapped with the main peak of the $^2B_1$ state. We expected that the Frank–Condon factors for the transition to the $^2B_1$ state should be similar to those of the $^2A_1$ state.

C. Observation of the C–C cleaved isomer: C_{60}–O–C_{60}^{2-}

The spectral features observed between 1.5 and 2.5 eV occurred in the energy gap region of $C_{120}O^{2-}$ and, in principle, could be due to shake-up processes. However, that seemed rather unlikely because according to our MCSCF calculations, the occupancy numbers of orbitals other than a_1 and b_1 were basically negligible in either of the spin states of

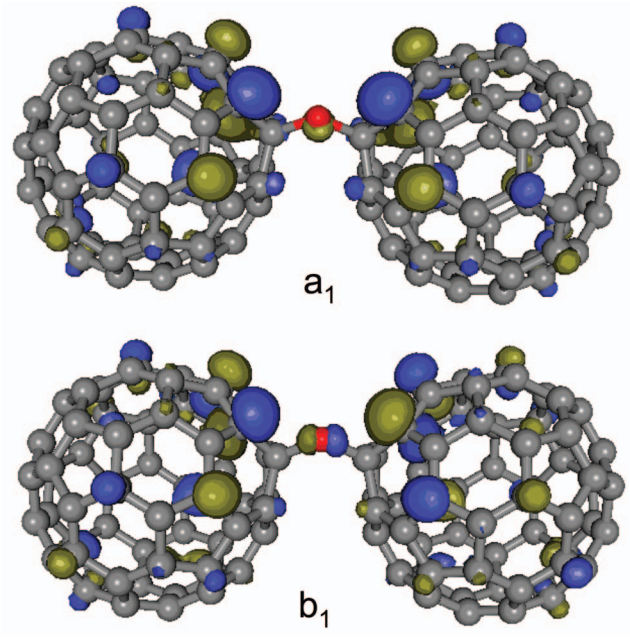

FIG. 5. (Color) Pictures of the highest occupied molecular orbital (HOMO) (b_1) and HOMO−1 (a_1) of the C–C bond cleaved C_{60}–O–C_{60}^{2-} isomer.

$C_{120}O^{2-}$. Alternatively, these features could come from isomers formed by the opening of the furan ring linking the two C_{60} units in $C_{120}O^{2-}$. Even though these isomers are much higher in energy, they could be produced during the electrospray and contribute to the PES spectra. The observation of abundant C_{60}^- and $C_{60}O^-$ in the mass spectra suggested that fragmentation of $C_{120}O^{2-}$ did take place readily in our electrospray source, giving further evidence for the existence of the ring-opened isomer.[35]

Particularly, our calculations showed that the C–C cleaved isomer, labeled as C_{60}–O–C_{60}^{2-} to distinguish it from the main furan-linked isomer, is only 36 kJ/mol higher in energy and would be the most likely carrier of the spectral features observed between 1.5 and 2.5 eV. This isomer would be expected to possess a higher electron binding energy than the main $C_{120}O^{2-}$ isomer, as observed experimentally, because the two C_{60} units are separated further, thus reducing the Coulomb repulsion in C_{60}–O–C_{60}^{2-}. Indeed, our calculations predicted an ADE of 1.4 eV for C_{60}–O–C_{60}^{2-}, in reasonable agreement with our observed ADE of 1.54 eV [Fig. 1(b)]. Furthermore, our calculations showed that the gap between the highest occupied molecular orbital (HOMO) and HOMO−1 in C_{60}–O–C_{60}^{2-} is 0.33 eV, which is in excellent agreement with the observed energy difference between the peak at 1.54 and 1.84 eV [Fig. 1(b)]. These results imply that the 1.84 eV peak represents the first excited state of the C_{60}–O–C_{60}^- monoanion. The fine features following the 1.54 and 1.84 eV peaks are probably due to vibrational excitations. Our DFT calculations revealed that the top two valence orbitals (Fig. 5) differ significantly from those of the furan-linked main isomer (Fig. 2). Both HOMO (b_1) and HOMO−1 (a_1) are fully occupied and are quite localized. The breaking of the C–C bond would create a diradical for the neutral C_{60}–O–C_{60} isomer. In the C_{60}–O–C_{60}^{2-} dianion, the extra electrons pair up with the single electron on each cage, giving rise to two fully occupied b_1 HOMO and a_1 HOMO−1 orbitals and resulting in a relatively stable dianion.

VI. CONCLUSIONS

In summary, we have reported high resolution and low-temperature photoelectron spectra of doubly charged anions of a fullerene dimer oxide ($C_{120}O^{2-}$) in conjunction with theoretical calculations to aid the spectral assignments and interpretation. Two structural isomers were observed in the dianion beam: The conventional and more stable furan-linked $C_{120}O^{2-}$ and a less stable C–C cleaved C_{60}–O–C_{60}^{2-} isomer produced during the electrospray ionization. Distinct vibrationally resolved photoelectron spectral features were observed for each isomer due to the cooling of the parent dianions in a cold ion trap. The second electron affinity of $C_{120}O$ was measured to be 1.02 ± 0.03 eV. A low-lying excited state was also observed for $C_{120}O^-$ at 0.09 eV above the ground state. The C_{60}–O–C_{60}^{2-} isomer was observed to possess a higher electron binding energy of 1.54 ± 0.05 eV due to the expected smaller intramolecular Coulomb repulsion. Theoretical calculations suggest that the two excess electrons in the $C_{120}O^{2-}$ dianion each occupy a C_{60} ball with very weak spin coupling.

ACKNOWLEDGMENTS

Part of this work done at Richland was supported by the U.S. National Science Foundation (CHE-0349426) and performed at the W. R. Wiley Environmental Molecular Sciences Laboratory, a national scientific user facility sponsored by DOE's Office of Biological and Environmental Research and located at Pacific Northwest National Laboratory, which is operated for DOE by Battelle. L.S.W. gratefully acknowledges the support of the Alexander von Humboldt Foundation, which makes this collaborative work possible. I.N.I. is thankful to the RFBR Grant No. 08-03-00626. M.M.K. acknowledges support by the Deutsche Forschungsgemeinschaft (DFG) as administered by the Karlsruhe Center of Excellence for Functional Nanostructures (CFN).

[1] R. L. Hettich, R. N. Compton, and R. H. Ritchie, Phys. Rev. Lett. **67**, 1242 (1991).
[2] L. S. Wang, J. Conceicao, C. Jin, and R. E. Smalley, Chem. Phys. Lett. **182**, 5 (1991).
[3] W. H. Green, Jr., S. M. Gorun, G. Fitzgerald, P. W. Fowler, A. Ceulemans, and B. C. Titeca, J. Phys. Chem. **100**, 14892 (1996).
[4] D. Dubois, K. M. Kadish, S. Flanagan, and L. J. Wilson, J. Am. Chem. Soc. **113**, 7773 (1991).
[5] R. C. Haddon, Acc. Chem. Res. **25**, 127 (1992).
[6] C. M. Varma, J. Zaanen, and K. Raghavachari, Science **254**, 989 (1991).
[7] S. Chakravarty, M. P. Gelfand, and S. Kivelson, Science **254**, 970 (1991).
[8] O. Gunnarsson and G. Zwicknagl, Phys. Rev. Lett. **69**, 957 (1992).
[9] R. L. Martin and J. P. Ritchie, Phys. Rev. B **48**, 4845 (1993).
[10] M. R. Pederson and A. A. Quong, Phys. Rev. B **46**, 13584 (1992).
[11] O. Gunnarsson, H. Handschuh, P. S. Bechthold, B. Kessler, G. Ganteför, and W. Eberhardt, Phys. Rev. Lett. **74**, 1875 (1995).
[12] S. Lebedkin, S. Ballenweg, J. Gross, R. Taylor, and W. Krätschmer, Tetrahedron Lett. **36**, 4971 (1995).
[13] A. B. Smith, H. Tokuyama, R. M. Strongin, G. T. Furst, and W. J. Romanow, J. Am. Chem. Soc. **117**, 9359 (1995).
[14] J. Zhang, K. Porfyrakis, M. R. Sambrook, A. Ardavan, and G. A. D. Briggs, J. Phys. Chem. B **110**, 16979 (2006).

[15] H. J. Eisler, F. H. Hennrich, E. Werner, A. Hertwig, C. Stoermer, and M. M. Kappes, J. Phys. Chem. A **102**, 3889 (1998).
[16] P. Paul, K. C. Kim, D. Sun, P. D. W. Boyd, and C. A. Reed, J. Am. Chem. Soc. **124**, 4394 (2002).
[17] S. C. Drew, J. F. Boas, J. R. Pilbrow, P. D. W. Boyd, P. Paul, and C. A. Reed, J. Phys. Chem. B **107**, 11353 (2003).
[18] X. B. Wang, C. F. Ding, and L. S. Wang, J. Chem. Phys. **110**, 8217 (1999).
[19] X. B. Wang, H. K. Woo, and L. S. Wang, J. Chem. Phys. **123**, 051106 (2005).
[20] X. B. Wang, H. K. Woo, B. Kiran, and L. S. Wang, Angew. Chem., Int. Ed. **44**, 4968 (2005).
[21] O. Hampe, M. Neumaier, M. N. Blom, and M. M. Kappes, Chem. Phys. Lett. **354**, 303 (2002).
[22] X. B. Wang, H. K. Woo, J. Yang, M. M. Kappes, and L. S. Wang, J. Phys. Chem. C **111**, 17684 (2007).
[23] S. A. Shaffer, K. Tang, G. A. Anderson, D. C. Prior, H. R. Udseth, and R. D. Smith, Rapid Commun. Mass Spectrom. **11**, 1813 (1997).
[24] D. N. Laikov, Chem. Phys. Lett. **281**, 151 (1997).
[25] D. N. Laikov and A. Yu. Ustynyuk, Russ. Chem. Bull. **54**, 820 (2005).
[26] J. P. Perdew, K. Burke, and M. Ernzerhof, Phys. Rev. Lett. **77**, 3865 (1996).
[27] O. T. Ehrler, F. Furche, J. M. Weber, and M. M. Kappes, J. Chem. Phys. **122**, 094321 (2005).
[28] X. B. Wang, H. K. Woo, X. Huang, M. M. Kappes, and L. S. Wang, Phys. Rev. Lett. **96**, 143002 (2006).
[29] A. A. Granovsky, PC GAMESS, Version 7.1 (http://classic.chem.msu.su/gran/gamess/index.html).
[30] A. Peluso, F. Santoro, and G. Del Re, Int. J. Quantum Chem. **63**, 233 (1997).
[31] R. Borrelli and A. Peluso, J. Chem. Phys. **119**, 8437 (2003).
[32] X. B. Wang, H. K. Woo, B. Kiran, and L. S. Wang, J. Phys. Chem. A **109**, 11089 (2005).
[33] X. B. Wang, C. F. Ding, and L. S. Wang, Phys. Rev. Lett. **81**, 3351 (1998).
[34] L. S. Wang, C. F. Ding, X. B. Wang, and J. B. Nicholas, Phys. Rev. Lett. **81**, 2667 (1998).
[35] A $[C_{60}^{-}\cdots C_{60}O^{-}]$ nonbonded adduct, similar to $(C_{60})_n(CN)_m^{x-}$ adducts observed previously [A. A. Tuinman and R. N. Compton, J. Phys. Chem. A **102**, 9791 (1998)], can be ruled out because it is expected to be energetically unfavored compared to the covalently bonded $(C_{60}-O-C_{60})^{2-}$ dianion.
[36] MOLEKEL visualization package (http://www.cscs.ch/molekel/).